

³Jones, R. M., "Comparison of Potential Electric Propulsion System for Orbit Transfer," *Journal of Spacecraft and Rockets*, Vol. 21, No. 1, 1984, pp. 88–95.

⁴Oleson, S. R., Myers, R. M., Kluever, C. A., Riehl, J. P., and Curran, F. M., "Advanced Propulsion for Geostationary Orbit Insertion and North-South Station Keeping," *Journal of Spacecraft and Rockets*, Vol. 34, No. 1, 1997, pp. 22–28.

J. A. Martin
Associate Editor

Spacecraft Thermal Analysis and Control by Thermal Energy Optimum Distribution

Marino Fragnito*

Groupe d'Etudes et de Conseils en Ingenierie,
06150 Cannes, France

and

Massimiliano Pastena[†] and Marco D'Errico[‡]
Second University of Naples, I-81031 Aversa, Italy

Nomenclature

| | | |
|-----------|---|--------------------------------|
| E_{IN} | = | energy for battery charge |
| E_{OUT} | = | energy needed from the battery |
| P_{BCR} | = | charge power |
| P_{SP} | = | power produced by solar panel |
| T_{eq} | = | equilibrium temperature |
| T_{req} | = | temperature requirement |

Subscripts

min, max = minimum, maximum value

Superscript

r = r th orbit

Introduction

THIS Note presents a new thermal design and control technique based on the concept of an optimum global thermal energy distribution, achieved by a successive model size increase through a critical substructuring method, using MATLAB® software codes, until NASTRAN finite element analysis and verification. Figure 1 shows the procedure flowchart, which consists of three main phases: system definition, thermal design, and detailed modeling and verification. The technique has been applied to the design of the SMART microsatellite, developed at the Universities of Naples under the sponsorship of the Italian Space Agency. SMART (450 × 450 × 360 mm stowed; 33 kg; 64-W average power) is a three-axis stabilized multimission microsatellite aimed at carrying remote sensing payloads on sun-synchronous orbits¹ with altitudes ranging from 400 to 1000 km. The in-orbit configuration of SMART is shown in Fig. 2.

Received 23 January 2001; revision received 26 September 2001; accepted for publication 27 September 2001. Copyright © 2001 by the American Institute of Aeronautics and Astronautics, Inc. All rights reserved. Copies of this paper may be made for personal or internal use, on condition that the copier pay the \$10.00 per-copy fee to the Copyright Clearance Center, Inc., 222 Rosewood Drive, Danvers, MA 01923; include the code 0022-4650/02 \$10.00 in correspondence with the CCC.

*Space Division Engineer, 5 Avenue St. Hubert.

[†]Research Engineer, Dipartimento di Ingegneria Aerospaziale, Via Roma 29.

[‡]Associate Professor, Dipartimento di Ingegneria Aerospaziale, Via Roma 29.

Technique Description

The different procedure subphases are described in the following subsections.

System Analysis

The first step is aimed at designing a suitable configuration. SMART design, mass, and dimensions were determined in order to guarantee compatibility with the majority of launch opportunity. The simplest solution was retained: bus of cubic shape with solar panels deployment consisting in a rigid rotation of the lateral surfaces around the deployment axis (Fig. 2). The flight configuration selection consists in computing the optimum deploying angles; the optimum condition is given by referring to both power and thermal requirements.

Environmental Modeling

To simulate satellite-environment interactions, a MATLAB code was developed.² Thermal inputs and electric energy can be computed for each configuration under analysis (i.e., for each couple of deployment angles θ_1 and θ_2).

Global Thermal Energy Estimation

At this level of design, thermal analysis is based on the preceding assumptions. Power analysis is carried out considering solar panel working at their maximum power point at the end of life and at worst condition, as it is assumed in electric power subsystem (EPS) design. Three orbits, during summer and winter solstices and spring equinox, corresponding to the extreme values of the sun angle, are selected for the analysis. The optimization procedure is based on the comparison of the electric power generated along the orbit with the power requirement. In particular, for each orbit and for each configuration two energies must be computed, as well as the minimum and maximum temperatures. A given configuration can be considered preliminarily acceptable if

$$\exists [P_{BCR,min}^r \quad P_{BCR,max}^r] \subset]0 \quad P_{SP,MAX}^r - P_L^r]: \forall P_{BCR}^r \in [P_{BCR,min}^r \quad P_{BCR,max}^r] \Rightarrow E_{IN}/E_{OUT} \geq 1 \quad (1)$$

and for each subsystem

$$[T_{eq,min}^r \quad T_{eq,max}^r] \subseteq [T_{req,min} \quad T_{req,max}] \quad (2)$$

Then, considering orbits in different periods of the year, the configuration can be selected only if

$$\bigcap_i [P_{BCR,min}^r \quad P_{BCR,max}^r] \neq \emptyset \quad (3)$$

The configuration (in the worst orbit case) giving the maximum value of $E_{IN,max}/E_{OUT}$ is chosen.

Results

The analysis has been based on SMART microsatellite power budget³ with orbital data derived by the Polar Satellite Launch Vehicle (PSLV) assuming a descending node local time of 1100 (Ref. 1). Solar panel performance are computed considering data of space qualified GaAs solar cells.³ Figure 3 shows three surfaces representing the value of the ratio E_{IN}/E_{OUT} for each configuration (θ_1, θ_2). Each surface has been computed for one of the three orbital cases considered.

Moreover, assuming a margin of 15% on E_{IN} , the 1.15 level curves for the three surfaces show that the number of acceptable configurations is minimum at the winter solstice and that the configurations which are acceptable during the winter solstice are also acceptable in the other cases. Among the acceptable configurations, the one that gives the maximum energy ratio is selected ($\theta_1 = 16$ deg and $\theta_2 = 90$ deg).

Spacecraft Thermal Substructuring

Once the geometrical configuration of SMART is set, a critical substructuring is performed. The exposed area-to-mass ratio can be assumed as a distinguishing parameter between the different parts of the spacecraft. Note that, at this stage, the thermal paths between

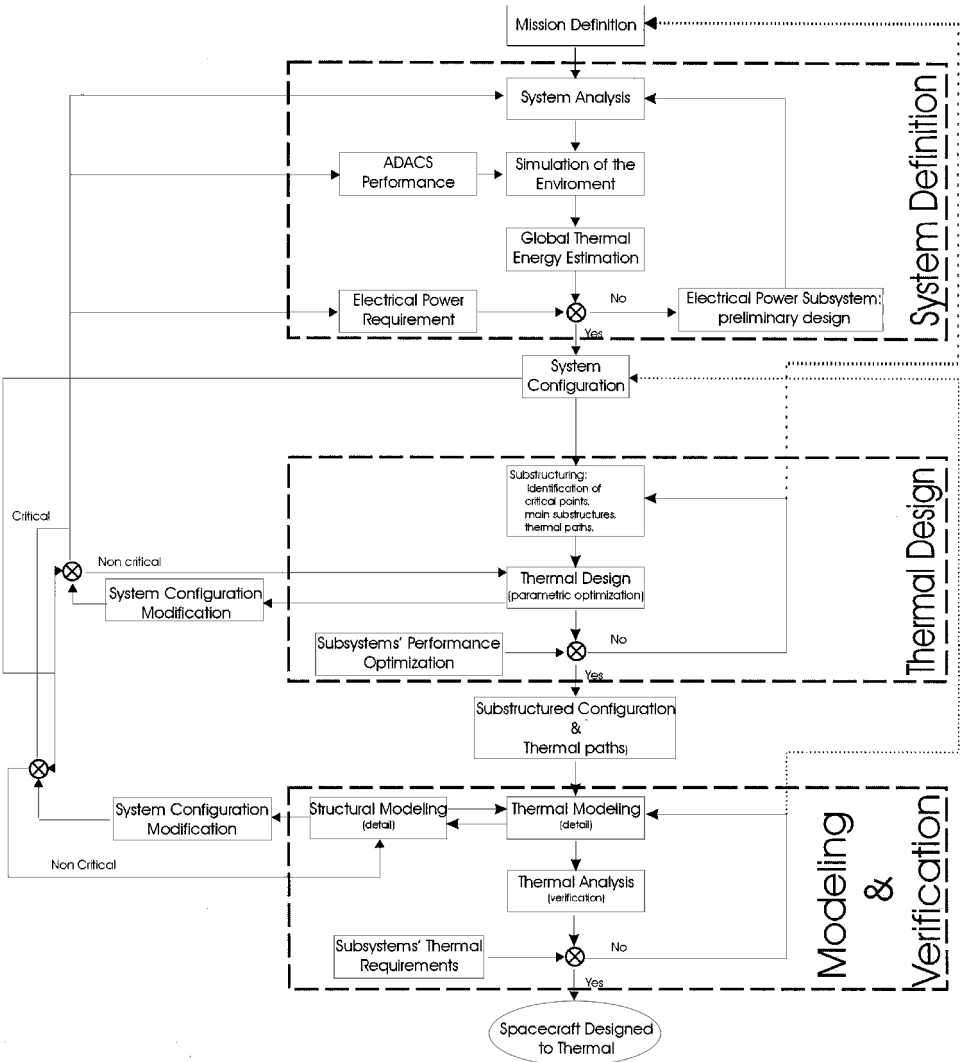


Fig. 1 Thermal design procedure flowchart.

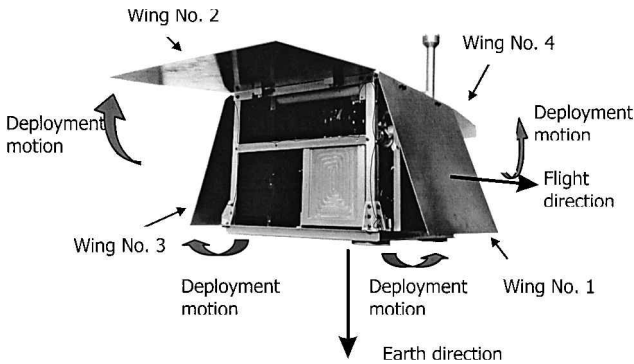


Fig. 2 SMART microsatellite in orbit configuration.

the spacecraft internal subsystems are mainly of a conductive kind. From these assumptions it descends that the geometry of the spacecraft can be simulated by five mathematical nodes: one to represent the main body and four to represent the deployable panels. Four main conduction paths can be assumed between the main body and each solar panel. The approach is based on the concept that the solar panels, because of their configuration, behave as radiators, when in shadow, and as thermal energy accumulators when exposed to the sun. Then, the amount of thermal energy, to be distributed within the satellite, depends on the properties of the back surface of the solar panels (solar cells have given absorptivity and emissivity) and on the values of the main conduction paths. To optimize the

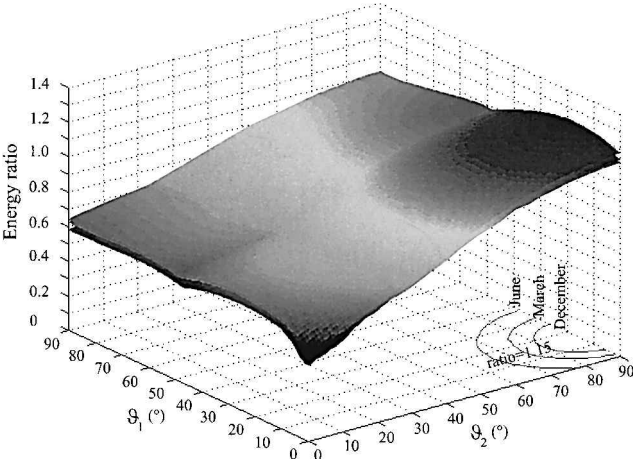


Fig. 3 Energy ratio vs the deployment angles.

thermal performance of each part of the spacecraft, a parametric analysis can be performed, using the substructured model, assuming the values of the conduction paths and the surface properties as parameters.

Parametric Optimization

The parametric optimization is performed on the basis of a transient thermal analysis of the five nodes spacecraft model in the orbital environment.⁴

The worst case was identified in the system definition phase as the cold case of the spacecraft operating life, occurring at the winter solstice, then the thermal design was addressed to optimize the performance in this worst condition. The spacecraft integrated thermal design goal is to meet the components temperature requirements while maximizing their performance. In particular, at the system substructure level, to optimize the performance means 1) to keep the solar array at the minimum possible temperature, compatible with the components requirements, with the minimum possible thermal excursion along the orbit; and 2) to limit the amplitude of the body temperature excursion and to keep its average temperature in the components operating temperature range.

The global system temperature excursion is dominated by the solar array temperature, which regulates the main body temperature through the main conduction of ad-hoc designed conduction paths. The parametric analysis is then based on an estimation of the solar

wing temperature, which is calculated as a function of the thermal conduction ($K = [W/K]$) of the path between the wings and the satellite main body and the absorptivity α and emissivity ε of the wing back surfaces. For each solar panel, among the control parameters, the α , ε , and K values that give a minimum temperature along the orbit of -54°C are considered, assuming a safety margin of 11°C above the minimum operating temperature of the solar array components (-65°C); these parameters are plotted as $\alpha(\varepsilon)$ curves, each curve related to a given K . Then, for each curve (and then for each K) the α and the ε values corresponding to the minimum amplitude of the orbital thermal cycling are chosen.

Finally the optimum K parameter (and the corresponding optimum values of α and ε) is chosen in order to have the minimum thermal excursion along the orbit.⁴ The theoretical optimum values are derived by the parametric analysis for α (0), ε (1), and K (1.04 W/K for the 16 deg deployed and 0.345 W/K for the 90 deg deployed). Then off-the-shelf coatings are selected (Alzac A-5, $\alpha = 0.18$, $\varepsilon = 1$), and K (0.98 W/K for the 16 deg deployed and 0.32 W/K for the 90 deg deployed) is recomputed as a function of real α and ε . In Fig. 4 the cold case system temperatures, calculated by the MATLAB code with the optimum control values, are shown.

Thermal Modeling

A detailed finite element model of the assembled satellite has to be built in order to perform structural and thermal verification on the basis of the launch and orbital environment respectively. The accuracy of the mesh detail is governed by structural analysis needs.

Figure 5 shows a temperature contour on the satellite finite element model at a time along the orbit. The main conduction paths, sized by the preceding parametric analysis, have been modeled in order to provide the design conduction to the four wings. The average power consumption of the subsystems (heat generations) assumed for the worst case finite element method simulation is considered.⁵

Thermal Analysis

Through a NASTRAN transient thermal analysis, the subsystem temperatures along a given number of orbits were calculated.⁵ The

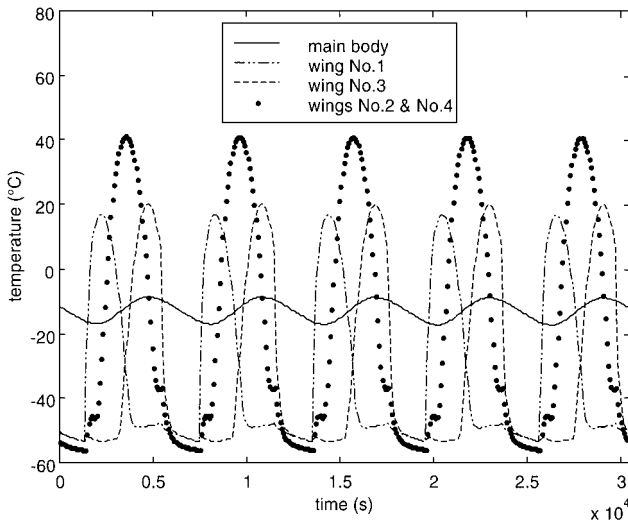


Fig. 4 Cold case system temperatures.

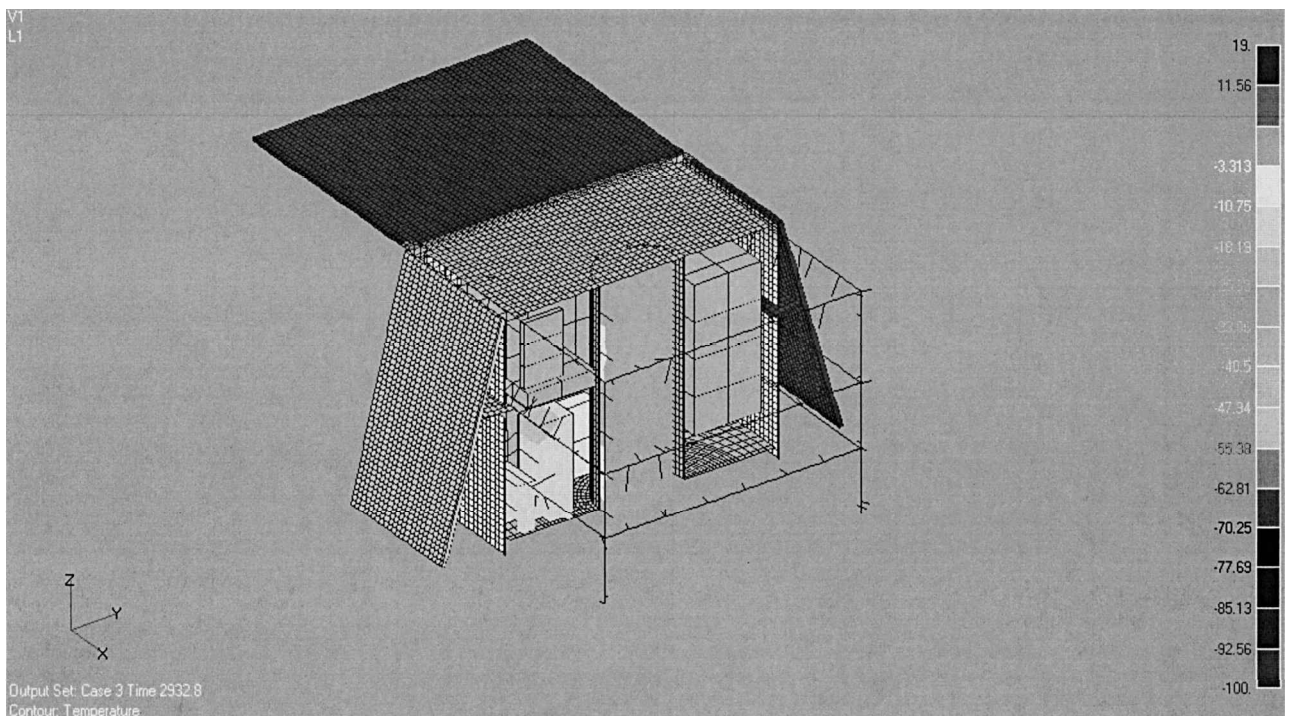


Fig. 5 Satellite temperature contour (section view) at a time along the orbit.

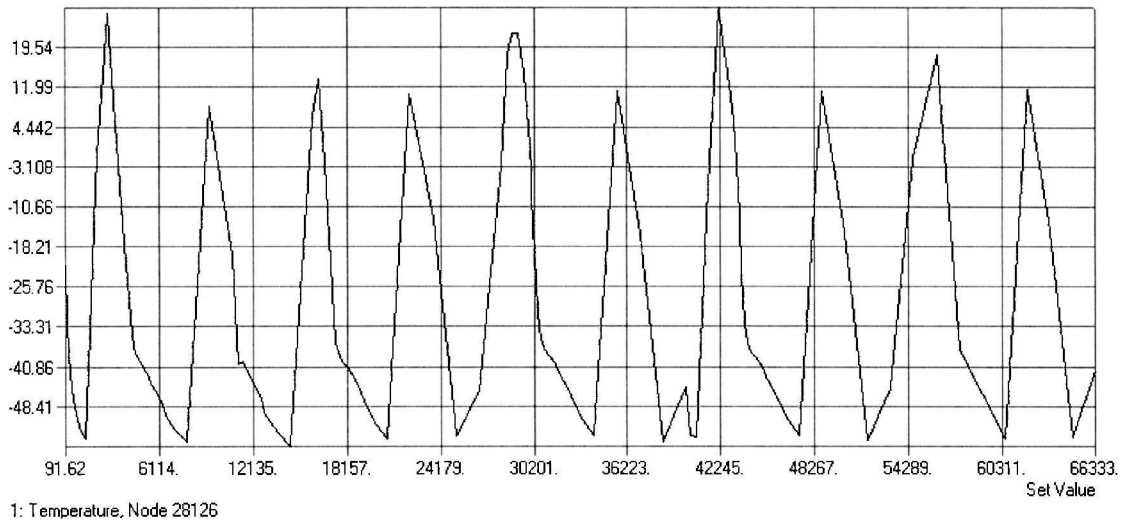


Fig. 6 Node 28,126 (16-deg deployed wing) temperature excursion along 10 orbits.

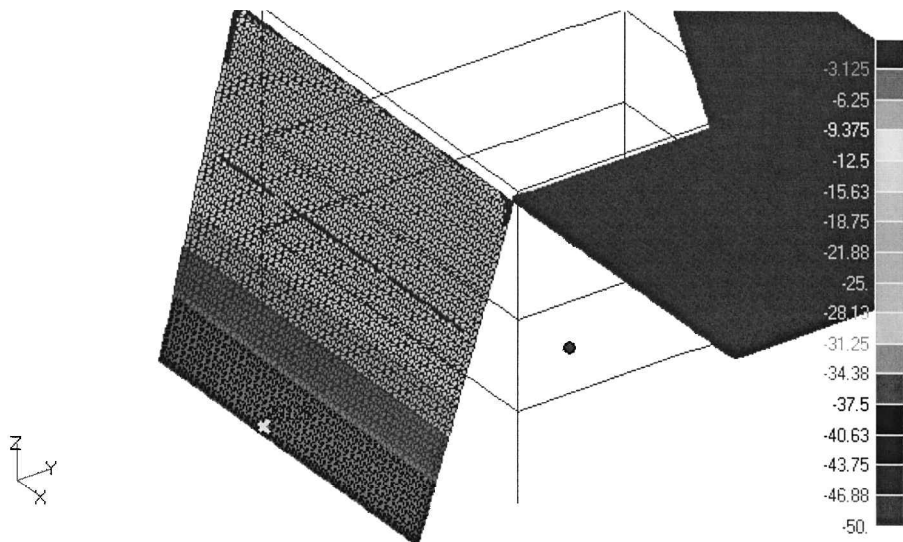


Fig. 7 The 16-deg deployed wing temperature contour (at a time along the orbit) and 28,126 node identification.

temperature variation on the solar wing node, which exhibits maximum excursion, is shown in Figs. 6 and 7 together with a temperature contour of the 16-deg deployed wing at a specific time along the coldest orbit.

Conclusions

In this Note a new thermal design and control technique was presented, based on a successive model size increase. Large-size thermal models were developed and analyzed in NASTRAN finite element environment, whereas small-size models were analyzed by ad-hoc-built MATLAB software. This choice was driven by the opportunity to achieve the peculiar advantages of the two approaches. NASTRAN finite element method based software allows both thermal and structural analysis by the same model and expertise; furthermore, data of large-scale models are easily managed by means of the finite element method pre- and postprocessing tools. On the other hand, in order to gain full advantage of MATLAB environment flexibility, small-size models were analyzed by means of MATLAB codes. External subroutines, such as orbit and attitude propagators and EPS performance analyzers, were integrated in the thermal code. Small-size models were allowed to optimize the interactions between the thermal and the other subsystems, giving a reference solution for the larger models. In conclusion, the Note showed that an ad-hoc schematization of thermal analysis and design in succes-

sive phases was allowed to achieve a number of goals before the use of NASTRAN for the detailed final verification. Small-size models were allowed to identify and control the effect of design choices on the overall design of the SMART microsatellite.

References

- ¹D'Errico, M., and Vetrella, S., "Mission Analysis of an Earth Observation Microsatellite," International Astronautical Federation, Paper 97-B.3.01, Oct. 1997.
- ²D'Errico, M., Grassi, M., and Vetrella, S., "A Bistatic SAR Mission for Earth Observation Based on a Small Satellite," *Acta Astronautica*, Vol. 39, No. 9-12, 1996, pp. 837-846.
- ³D'Errico, M., and Pastena, M., "Solar Array Design and Performance Evaluation for the SMART Microsatellite," International Astronautical Federation, Paper 98.R.1.06, Oct. 1998.
- ⁴Fragnito, M., and Pastena, M., "Design of Smart Microsatellite Deployable Solar Wings," *Acta Astronautica*, Vol. 46, No. 2-6, 2000, pp. 335, 344.
- ⁵Fragnito, M., "SMART Microsatellite Structure, Mechanisms and Thermal Design," *Proceedings of the 5th International Symposium on Small Satellites Systems and Services*, Centre National d'Etudes Spatiales, La Baule, France, June 2000, p. 10.